COMPDYN 2015
5th ECCOMAS Thematic Conference on
Computational Methods in Structural Dynamics and Earthquake Engineering
M. Papadrakakis, V. Papadopoulos, V. Plevris (eds.)
Crete Island, Greece, 25–27 May 2015

DEVELOPMENT OF A HYBRID SYSTEM FOR IDENTIFICATION OF ELASTIC MATERIAL IN COMPOSITE LAMINA: APPLICATION OF LAMB WAVES AND NEURAL NETWORKS

Zenon Waszczyszyn [1*], **Piotr Nazarko** [2],
Pawel Packo [3], **Lukasz Ambrozinski** [3] **and Tadeusz Uhl** [3]

[1] Cracow University of Technology,
Institute for Computational Civil Engineering,
Warszawska 24, Cracow 31-155, Poland,
e-mail: zenwa@L5.pk.edu.pl

[2] Rzeszow University of Technology,
Chair of Structural Mechanics,
Powstancow Warszawy 12, 35-959 Rzeszow, Poland
email: pnazarko@ prz.edu.pl

[3] AGH University of Science and Technology,
Chair of Mechatronics and Robotics
Al. Mickiewicza 30, 30-059 Cracow, Poland
email: {pawel.packo, ambrozine, tuhl}@agh.edu.pl

Keywords: Hybrid Computational System, Structure Health Monitoring, Lamb waves, Dispersion Curve, Lamb DC, Artificial Neural Network, direct analysis (simulation), reverse analysis (identification), parameter identification.

Abstract. *A new Hybrid Computational System is presented, developed for the identification of homogeneous, elastic, hexagonally orthotropic plate parameters. Attention is focused on the construction of dispersion curves, related to Lamb waves. The main idea of the hybrid system lies in the separation of two essential basic computational stages, corresponding to the direct and inverse analyses. In the frame of the first stage an experimental dispersion curve DC_{exp} is constructed, applying Guided Wave Measurement technique. The other stage is supported on the application of artificial neural network trained 'off line'. Two case studies are presented, corresponding either to pseudo-experimental computer simulations or to laboratory tests.*

1 INTRODUCTION

The presented paper is related to a new area of science and technology, called Structure Health Monitoring (SHM). It has been increasingly developing for some time now. SHM deals with structures and various processes closely connected with the life and maintenance of a variety of engineering structures. An important role for SHM is played by systems which on the base of monitoring or measurements can reflect the actual state (health) of structures. This permits control of the structure and warning against failures or dangerous events. Non-destructive methods of structure examination and 'on line' methods of information transmission are especially valuable for aspect of SHM, see, e.g. [1, 2, 3].

From among non-destructive methods, the application of ultrasonic waves is worth emphasizing for the evaluation of material properties and detection of various defects, cf, references in [2]. In what follows we are discussing a comparatively simple problem of the application of the Lamb Waves (LWs) propagation in thin, elastic and homogeneous plates, cf. [4-6]. These waves are guided in the vibration plane, perpendicular to the plate mid-surface and are propagated over a comparatively long distance.

The presented paper is related to the identification of parameters of anisotropic plates. The formulation of mathematical models of such plates and the identification of 'a priori' unknown parameters or defects is much more difficult than in isotropic plates. In such a situation we can tread the solutions obtained for isotropic plates as a special case, called even "bench mark" solutions for the analysis of orthotropic plates.

The Lamb equations make it possible to formulate the Dispersion Curve (DC). A relation $k(f \mid \mathbf{par})$ can be written, where: k – DC wavenumber, f – frequency of vibrations as an independent variable, **par** – vector of plate parameters. For example, in the case of isotropic, homogeneous plate, this vector is completed from the following constants: **par** = $\{E, \nu, \rho, d\}$, where: k and ν, – Young's modulus and Poisson ratio, ρ and d – plate density and thickness, respectively.

Unfortunately, the Lamb equations can be derived in an implicit and very elegant form (see e.g. books [4, 5] for the case of isotropic plates), but they can be analysed only by numerical methods. There is a variety of such numerical methods based on FEM, BEM and FDM. What seems especially numerically efficient are their modifications and combinations, see e.g. LISA/SIM (Local Interaction Simulation Approach/ Sharp Interface Model), EFIT (Elasto-dynamic Finite Integration Technique), see [7-11]. Unfortunately, these methods are rather "numerical costly" since they need a great number of numerical operations.

What seems to be especially numerically efficient, there is the formulation of semi-analytical methods (SEM) as the application of EFIT/LISA/FDM, with introducing of the Finite Difference Method (FDM) , see [12-14]. Unfortunately, the above listed methods are rather numerical costly since they need a great number of numerical operations.

Another disadvantage of the application of the aforementioned methods appears in the identification analysis, called in mathematics as the reverse approach.

This approach is related to the application of the paradigm of minimizing the difference between the "distance" between known and search states. Let us take as an example the norm of the experimental and numerically simulated values of the dispersion curves:

$$\left\| k_{num}^{(it)} - k_{\exp} \right\| \xrightarrow{it} \cong 0 \ . \tag{1}$$

In fact, the described approach, called in literature Classical Method (CM) of optimization, is refers to a sequence of direct problem solutions, see [14]. In our paper [15] we developed another approach, based on the application of Artificial Neural Networks (ANNs). This ap-

proach is related to the formulation of a corresponding Hybrid Computational Method (HCM). The system is composed of two stages. Stage A relates to the physical tests on material models (laboratory tests or measurements on laboratory models or structures). In Stage B data, satisfying the Lamb equations, are identified by 'off line' trained ANN. Then, preprocessed data of the Stage A are substituted as inputs into the trained network. Thus, the proposed HCS works 'numerically on line' as a method of one substitution of data from Stage A to Stage B.

The sketched HCM was checked in paper [15]. The results, obtained in this paper can also serve us as a "bench mark" in validation of our proposal. The main goal o our paper is a generalization of the approach developed in [15] to the appropriate modification of HCS for the identification of parameters for elastic orthotropic composite materials. In the present paper we adopted a hexagonal (five parameters) orthotropic material, corresponding to the unidirectional reinforced composite lamina.

Obviously, the identification of composite parameters is much more complicated than this applied for the isotropic material. Instead of the Armikulova's dimensionless Lamb equations, see [17], used for isotropic material, we now apply the finite difference equations, formulated in [13]. These equations have been adopted for computing patterns for the orthotropic material in Stage B for generating patterns needed for the 'off line' training and testing ANN as a component of HCS.

The basics on Lamb waves, and corresponding equations for the analysis of a thin plate made of hexagonally orthotropic material, are presented briefly.

Next, case studies are discussed. The first case refers to pseudo-experimental verification of the identification results, supported on data taken from [4] for hexagonally orthotropic plate. The other case study relates to data taken from laboratory tests on unidirectional reinforced composite lamina, see [17]. In both case studies the results of an extensive numerical analysis are connected with the sensitivity of Lamb dispersion curves to variations of material parameters.

2 LAMB WAVES IN ELASTIC THIN PLATES

2.1 Some basics of LW equations

The Lamb plane of vibrations is shown in Fig. 1.

a)

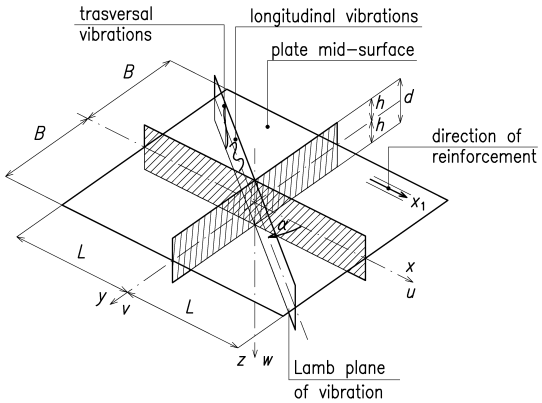

b)

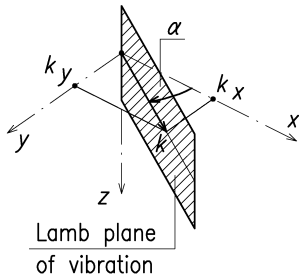

Figure 1: a) Lamb waves propagations with longitudinal, transverse and shear horizontal waves, b) Inclination angle α of vector wave-number $\mathbf{k}$ from reinforcement direction x_1

Fig. 2 illustrates the influences of displacements normal to the plate mid-surface which cause the symmetric and anti-symmetric modes of vibrations. These vibration modes can be drawn as radial in-plane and out of-plane motions, see [5].

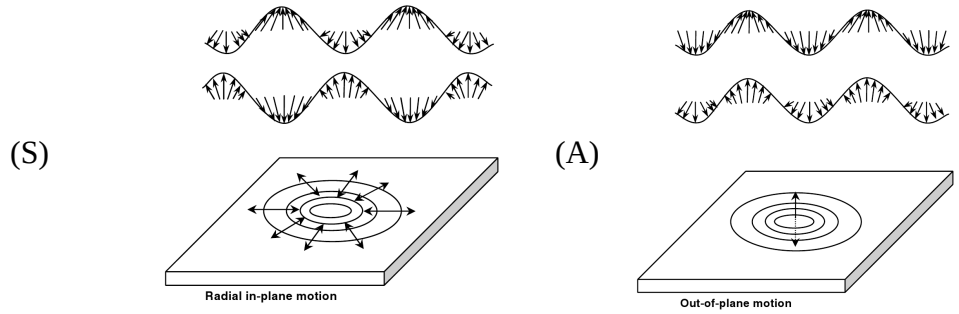

Figure 2. LW modes: (S) Symmetric (radial in-plane motion), (A) Anti-symmetric mode (out of-plane motion)

The adopted elastic, hexagonal, orthotropic material, has five independent elastic constants. The stiffness matrix of this material is shown in Table 1.

$\mathbf{C}_{(6x6)} =$

C_{11}	C_{12}	C_{12}			
C_{12}	C_{22}	C_{23}= $= C_{22} - 2\,C_{44}$			
C_{23}	C_{23}	C_{22}	C_{44}		
				C_{55}	
					C_{55}

Table 1: Stiffness matrix for hexagonal orthotropic material with 5 independent constants

The stiffness matrix of this material corresponds to the unidirectional reinforced composite lamina, see [11].

Two equations, which are the basis for deriving of Lamb equations, are: i) eigenvalue problem equations and ii) dispersion equations cf. e.g. [1, 5, 16].

2.2 Eigenvalue equations for composite lamina

The Cartesian coordinate system is adopted with *z* axis normal to the midsurface of a composite lamina, see Fig. 1. The displacement vector has components on the z distance to the plate midsurface:

$$\mathbf{W} \equiv \{u, v, w\} = \{U(z),\, V(z),\, W(z)\}\, \mathrm{e}^{[(k_x + k_y) - \omega t]} \equiv W\, \mathrm{e}^{\,i[(k_x + k_y) - \omega t]}, \tag{2}$$

where: $\mathbf{k} = [k_x, k_y]^{\mathrm{T}}$ – wave number vector of length $k = |\mathbf{k}| = +\sqrt{k_x^2 + k_y^2} = \omega / c_p$ and ω is angular frequency, c_{p} is phase frequency. The direction of wave propagation depends on the angle α, i.e. $\mathbf{k} = k[\cos\alpha, \sin\alpha]^{\mathrm{T}}$, k_x^2, see Fig. 1b.

The displacement functions (2) can be separated into symmetric and snit-symmetric modes, see [18].

$$U_{\mathrm{s}} \cos\xi z = C_1 \cos\xi z, \quad V_{\mathrm{s}} \cos\xi z = C_2 \cos\xi z, \quad W_{\mathrm{s}} \sin\xi z = C_1 \sin\xi z, \tag{3S}$$

$$U_a \cos\xi z = C_1 \sin\xi z, \quad V_a \sin\xi z = C_2 \sin\xi z, \quad W_{\mathrm{a}} \sin\xi z = C_3 \cos\xi z, \tag{3A}$$

where: ξ_j – eigenvalues that will be computed as solutions of the characteristic equations of the eigenvalue problem

2.3 Eigenvalue equations for composite lamina

From the equations of motion, see [18], we can formulate the following equations of the eigenvalue problem:

$$\mathbf{[\Gamma - \chi^2 I]\, C^T} \equiv \begin{bmatrix} \Gamma_{11} - \chi^2 & \Gamma_{12} & \Gamma_{13} \\ \Gamma_{12} & \Gamma_{22} - \chi^2 & \Gamma_{23} \\ \overline{\Gamma}_{13} & \overline{\Gamma}_{23} & \Gamma_{33} - \chi^2 \end{bmatrix} \begin{bmatrix} C_1 \\ C_2 \\ C_3 \end{bmatrix} = \begin{bmatrix} 0 \\ 0 \\ 0 \end{bmatrix}, \tag{4}$$

where: $\chi^2 = \rho\omega^2$, ρ^2 is the plate density. The expressions for Γ_{ij} can be found in [??]. For instance $\Gamma_{11} = C_{11}k_x^2 + C_{66}k_y^2 + C_{55}\xi^2$.

Characteristic equations related to the eigenvalue analysis Eq. (4) leads to the 6-the order algebraic equations, which can be solved only by means of numerical methods. That is why we apply the finite difference method, see [13], related to the LINSA system, see Appendix.

The Lamb wave equations are derived from the boundary conditions:

$$\sigma_z(\xi z)_{|z=\pm h} = 0, \quad \tau_{zx}(\xi z)_{|z=\pm h} = 0. \tag{5}$$

From the condition of existence of a non-trivial solution of the set of homogeneous equations (5) the dispersion Lamb function can be found. It has the following implicit form, see [18]:

$$F(k, f, C_{ij}, \chi^2, S \vee A) = 0. \tag{6}$$

3 BASIC ALGORITHMS FOR PLATE PARAMETERS IDENTIFCATION

3.1 Four essential algorithms for GWM

In the Guided Wave Monitoring or Measurements (GWM) four essential steps can be distinguished, see [2]. The steps are sketched in Fig. 3, underlining Step IV.

Steps I and II correspond to carrying out the experimental test and initial processing of measured responses (signals).

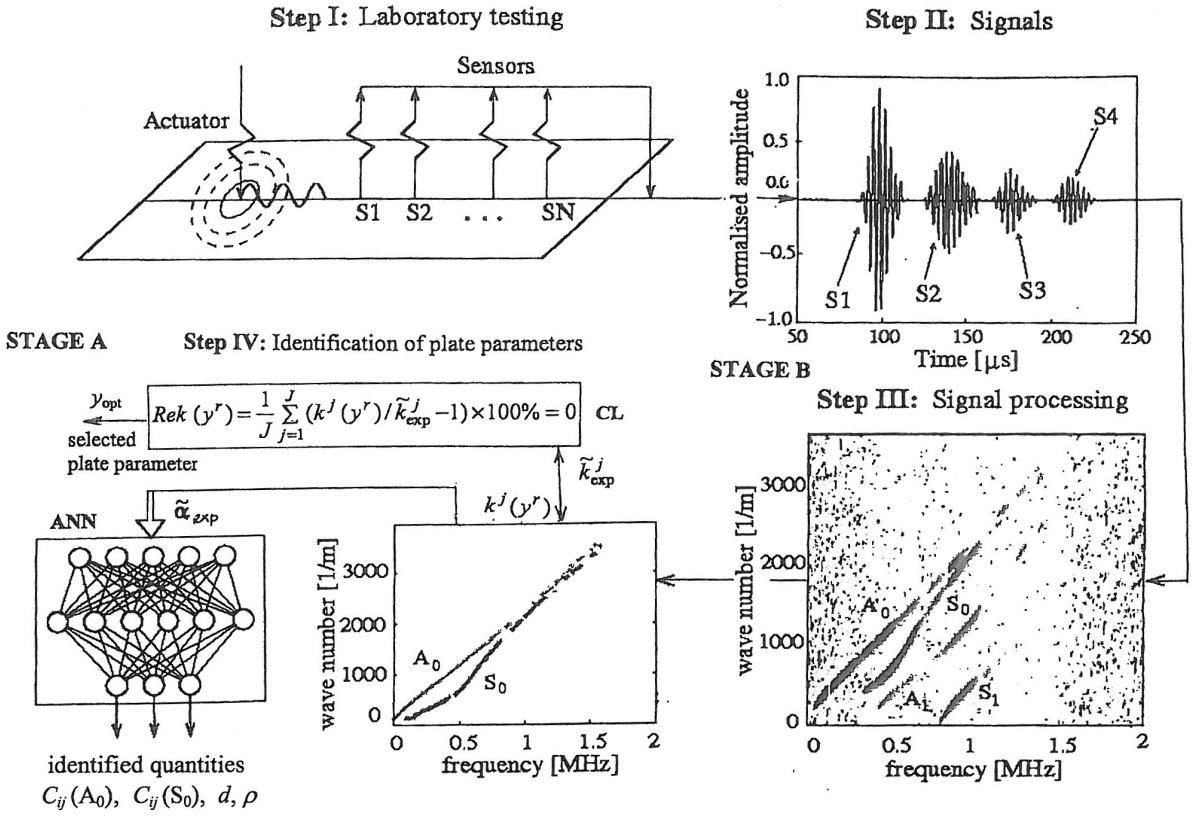

Fig. 3. Four essential steps for identification of plate parameters, applying Lamb wave measurement technique and identification procedures in step IV: CL –Classical approach, ANN – artificial neural network

Step III contains signals processing, applying B-scanning and 2D-FFT transformation [19]. The estimated local maxima on the plane (*f*, *k*) enable us to trace the dispersion curves. In Fig. 3 there are shown DCs, which fulfill symmetric and anti-symmetric modes of DCs. They are, in fact, a set of points $\{f_m^j, k_m^j\}_{j=1}^J$, where $m = 0, 1, 2, \ldots$ are numbers of vibration modes.

Step IV starts from the selection of points which are simulated by numerical methods. In the case presented in Fig.2 only the points related to modes A_0 and S_0 are shown.

This point is based on algorithms developed in [15] for elastic, isotropic plate parameters identification. In the present paper we have introduced some modifications, corresponding to the identification of elastic, hexagonal orthotropic material, see Table 1.

3.2 Hybrid Computational System and corresponding procedures

The Hybrid Computational System is composed of two computational Stages A and B, see Fig.3. Stage A is devoted to the testing analysis, to testing and processing of experimental data. Stage A corresponds to the direct analysis. Step B deals with the inverse analysis, starting from the extended Essential Step IV, see Fig. 3. In beginning the dispersion curves are selected from the spectrum of modes, shown in Essential Step III. In Fig. 3 the selection of two vibration modes was made, corresponding to modes A_0 and S_0.

The basic roles in reverse analysis plays ANNs, see [5, 20-22].The algorithms of Stage B were developed in [15]. In the present paper we discuss briefly only the main algorithms taken from paper aforementioned.

3.2 Algorithms of HCS

In our paper we have decided to restrict our analysis to a range of dispersion curves (DCs), since the considered composite lamina are adopted to be after numerical homogenization and material parameters are constant along the plate length 2 *L*, see Fig. 1. The adopted reference range is related to frequencies of excited vibrations, i.e. $f_{\text{ref}} \in [\, f_{\min}\, ,\, f_{\max}\,]$. The values and forms of corresponding points of experimental curves are processed in order to have experimental approximate dispersion curves related to the formulation processes. The value of f_{ref} is taken from laboratory tests. After numerical processing, an approximate vawenumber function $k_{\exp}\,(f \,|\, \mathbf{par})$ is obtained. In what follows the formulated dispersion curves can be written shortly in the form $k\,(\text{X}|\text{Y})$, where: X – independent variable, Y – given values of other variables.

In the presented paper we are discussing hexagonal orthotropic material with the stiffness matrix **C** shown in Table 1. In such a special case, the vector of identified plate parameters is $\mathbf{spar}_{(6\times 1)} = \{C_{11}, C_{22}, C_{44}, C_{66}, C_{12}, d\}$. The following parameters are fixed: $\rho_{\,fixed}$ – density of plate, *N* = number of station in the FDM formulas, see Appendix.

3.2.1 Simulation computation in Stage A

Stage A corresponds to the standard procedure, related to Guided Wave Monitoring GWM) technique, discussed in many books and papers, e.g. see references in [4, 5]. The main attention is focused on Stage B.

After evaluation of reference range $f_{ref}^{\exp}$ for selected modes vibrations, a set of experimental data can be completed.

$$\mathsf{D}_{\exp} = \{\, f^j,\, k^j \,|\, m \,\}_{j=1,\; m=1}^{J,\; M}, \tag{7}$$

where: $j = 1, 2, \ldots, J$ – numbers of dispersion points, m – numbers of vibration modes.

On the basis of data, approximate experimental curves can be formulated. The parameters of these curves are computed by means of the Least Squared Method (LSM):

$$\tilde{k}^{(M=2)} = \left(f \,|\, \mathbf{BF}_{\text{ref}}\,(f), D_{\exp} \right) \xrightarrow{\;LMS\;} \tilde{\boldsymbol{\alpha}}_{\exp}\,. \tag{8}$$

In the presented paper, $M = 2$ modes are adopted, i.e. A_0 and S_0. The reference basis function vector $\mathbf{BF}_{\text{ref}}\,(f)$ should corresponds to the adopted reference range $f_{\text{ref}} \in [\, f_{\min}\, ,\, f_{\max}\,]$ and to shape of the dispersion curve, represented by computed values of vector $\tilde{\boldsymbol{\alpha}}_{\exp}$. Components of this vector correspond to internal parameters, which control the transition from Stage A to Stage B.

3.2.3 Identification computation in Stage B

The main part of the stage B corresponds to an ANN, which is a solver of the inverse problems of identification of the plate parameters. Similarly as in [15].the Multi Layered Perceptron (MLP) network, see Haykin [24], of the following architecture can be designed:

$$\text{MLP: } \boldsymbol{\alpha}_{(I\,\times 1)} – \mathbf{H}_{(H\times 1)} – \mathbf{spar}_{(3\times 1)}\,, \tag{9}$$

where: I – number of inputs, H – number of sigmoid functions in the hidden layer designed.

The corresponding set P , composed of P pattern pairs, was adopted for the training of the MLP neural network from the view point of the identification purposes:

$$\mathrm{P} = \{\boldsymbol{\alpha}^p, \mathbf{t}^p = \mathbf{spar}^p\}_{p=1}^{P} . \tag{10}$$

The input vectors $\boldsymbol{\alpha}^p$ can be computed for Armirkulova's approximation in case of isotropic material of the plate, see [17] .We can start from a cloud of P points (f^p, k^p), fulfilling the Lamb dimensionless equations.

In case of the considered orthotropic material, instead of Armikulova's formulas the Finite Difference Method was adopted, see Appendix. These equations can be related to known target values $\mathbf{t}^p$ and the LSM method is applied for the anisotropic materials, computing the p-the input patterns:

$$k \left(f \,|\mathbf{BF}_{\mathrm{ref}}(f), \mathbf{spar}^p \right) \xrightarrow{LMS,\ FDM} \boldsymbol{\alpha}^p . \tag{11}$$

The patterns of the training set are selected from reference ranges of the output vector components of the output vector $\mathbf{spar}^p$. After the training of MLP, relative errors of the neural approximation can be computed:

$$Rey = \frac{1}{P} \sum_{p=1}^{P} (1 - y^p / t^p) \times 100\% \ , \tag{12}$$

where: y and t are computed and target values of the vector **spar** components**.**

The values of components of the vector of experimental curve parameters (11) are substituted into the trained MLP for computing:

$$\tilde{\boldsymbol{\alpha}}_{\mathrm{exp}} \xrightarrow{LMS} \mathbf{spar}_{\mathrm{MLP}} . \tag{13}$$

It should be emphasized that the identification computations in the Stage B are carried out 'off line'. Thus, solution (13) is obtained by patterns corresponding to the exact Lamb dispersion curves. It equals $\mathbf{spar}_{\mathrm{MLP}}$, with the accuracy corresponding to the MLP network errors (12). Thus, we can conclude that

$$\mathbf{spar}_{\mathrm{MLP}} = \mathbf{spar}_{\mathrm{ident}} \approx \mathbf{spar}_{\mathrm{exact}} , \tag{14}$$

The formula (14) gives identification in one substitution, without any iteration. We can call this approach the 'numerically on line' process.

4 CASE STUDIES

4.1 Identification of a pseudo-experimental hexagonal orthotropic composite

In this case study, the material constant values shown in Table 1, were taken from [4]:

C_{11} = 128.2 GPa, $C_{22} = C_{33}$ = 14.95 GPa, C_{44} = 3.81, GPa, $C_{55} = C_{66}$ = 6.73 GPa,
$C_{12} = C_{13}$ = 6.90 GPa, $C_{23} = C_{22} - 2\,C_{44}$ = 7.33 GPa, and ρ = 1.58 g/cm^3, N = 9, (15)
where: N – number of FD stations along the plate thickness.

Data (15) were applied in HCS for three excitations related to different direction of the Lamb planes, see Fig.: 1) $\alpha = 0^{\circ}$, $k_x = k$, $k_y = 0$, 2) $\alpha = 90^{\circ}$, $k_x = 0$, $k_y = k$, 3) $\alpha = 45^{\circ}$, $k_x = k_y = k$.

The computations were made for the reference range $f_{\text{ref}} \in [0.05, 0.5]$ MHz, see Fig. 4. In this Figure four LDCs modes are shown A_0 , SH_0, S_0 and A_1 for the Lamb planes $\alpha = 0^{\circ}$, 90° and 45°.

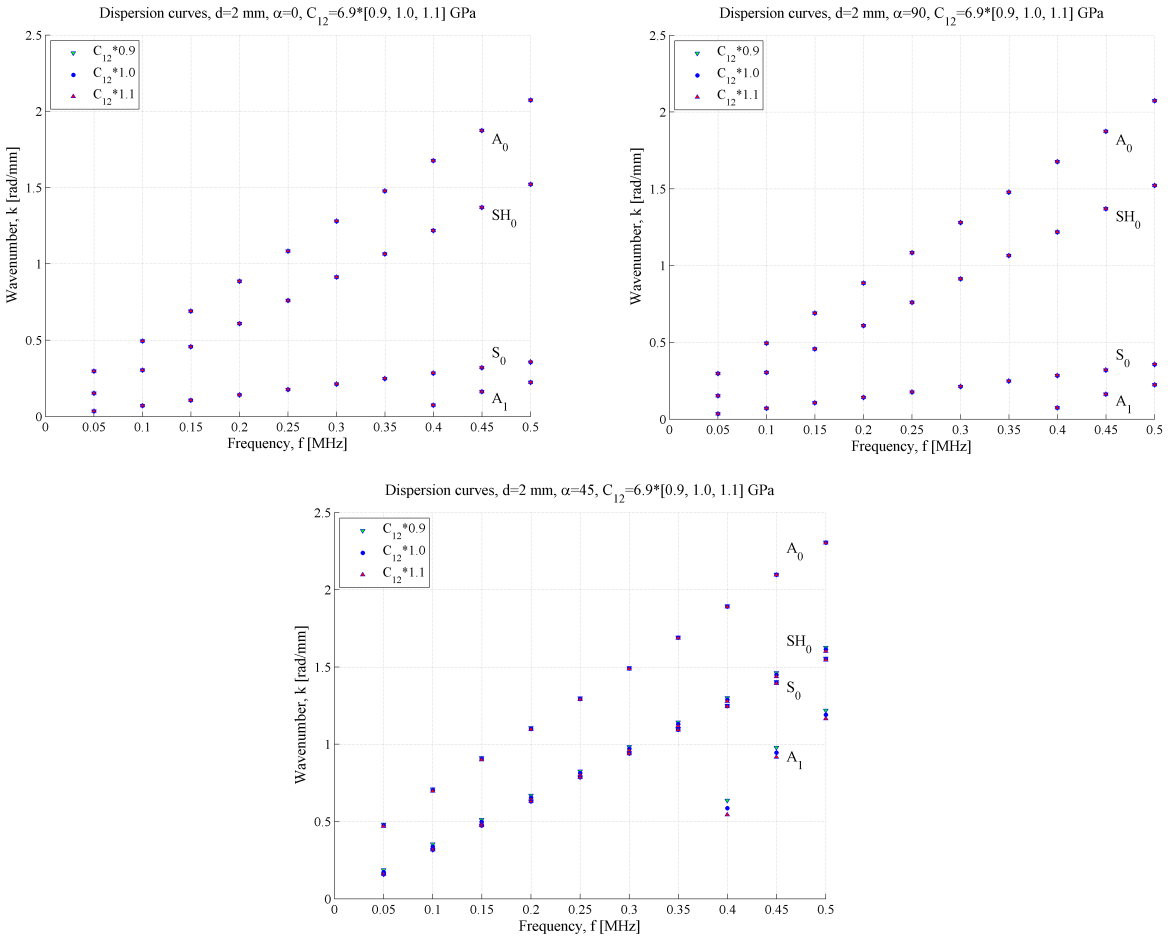

Figure 4. Sensitivity of modes A_0, SH_0, S_0 and A_1 for variations of material parameter C_{12}

The Shear Horizontal mode SH_0 is not dispersive and cannot be reconstructed by standard B-Scans techniques. The corresponding LDCs are close to straight lines. The dispersion curve is a linear functions, see [4], p. 244. The corresponding formula can be used for the calculation of the stiffness C_{66} value:

$$k = 2\pi\sqrt{\rho/C_{66}}\, f \quad \rightarrow \quad C_{66} = 4\pi^2 \rho\, (f/k)^2 \ . \tag{16}$$

For example, if we take the approximate value of wavenumber, $k \approx 1.52 \times 10^{-3}$ m^{-1}, then for $f \approx 0.5$ MHz the stiffness equals $C_{66} \approx 6.74$ MPa.

Similar sensitivity analysis was made for the other four parameters. The recognition of sensitivity of LDCs to perturbations by small values of plate parameters is indispensable for a proper selection of dispersion modes. Such recognition has been taken into account for evalu-

ation of reference ranges of the hexagonal, orthotropic material parameter variations in order to prepare patterns for ANNs training.

The carried out identification of data (15) taken from [4], and treated in the present paper as pseudo-experimental data, gave identified values very close to those in the above mentioned paper.

4.2 Identification by HSM on the base of a laboratory test

Let us start from the Stage A , Essential Step III, see Fig. 3. There are presented Scan-B maps in which LDCs as local maxima, found in the 2D-FTT transform space, see [19]. Corresponding curves were measured on carbon fiber reinforced plastic (CFRP). The Lamb waves propagated in directions α = 0º, 90º and 45º, corresponding to modes A_0, B_0 outlines of A_1 mode.

According to remarks in the previous Case Study, DC of SH_0 could not be reconstructed because it is related to a non-dispersive wave.

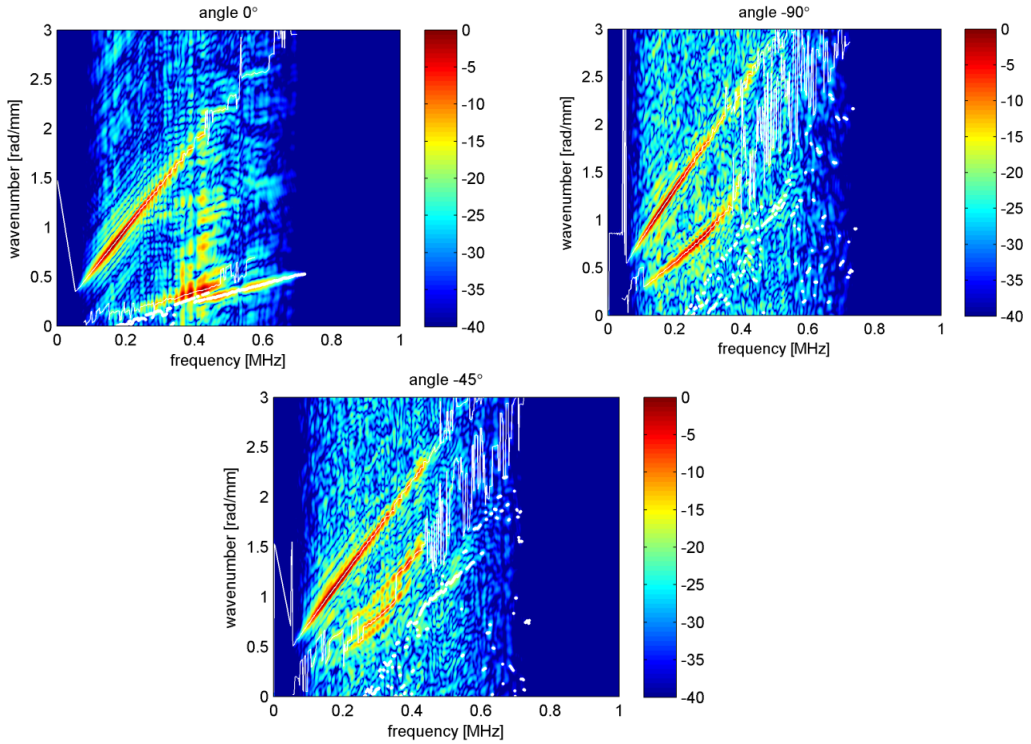

Figure 5. B-Scans and Diffusion Curves in α = 0º, 90º and 45º 2D-direction of vibration in FFT transform space for unidirectional reinforced composite lamina

It is visible that LDCs can be recognized in the reference range $f_{ref} \in [f_{min}, f_{max}]$. Moreover, the CDs shape can be reconstructed in an analytical form with an inaccuracy. We can apply the straight, sloppy lines as approximate LDCs. Such an approximation corresponds to the application of a single basis functions $k(f)$ for $f \in$ [0.2, 0.35] MH, see Fig. 6.

Then we can perturb a selected identified parameter and observe which mode is more sensitive to parameter perturbation.

In this study case, see Fig.6a, the perturbation of the stiffness C_{11} causes larger changes of the mode S_0. Now we can construct a set of points corresponding to 20 regularly placed station

f_j for $j = 1, \ldots, J$. For R changes of the stiffness $C_{11,r}$ we have $J \times R$ patterns for finding an optimal of parameter C_{11} by means of the Mean Square Method.

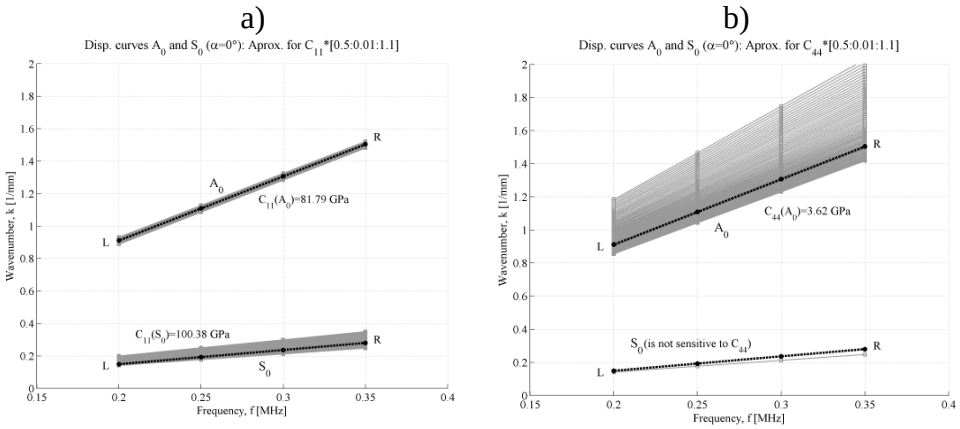

Figure 6. Sensitivity of modes A_0 and S_0 to changes of plate stiffness C_{11} and C_{44}

Optimal value of the parameter C_{11} can be also found by means of the mode A_0 .Similar perturbations of other parameters can points out which of optimal solutions is proper.

There no doubt that in case of identification of the parameter C_{44} the identification by means of the mode A_0 is better than by S_0.

The approach discussed above fully corresponds to the general method discussed in Point 3.2.3, where the basis functions (BF) are used. In the considered case study a straight BF is used with the left and right bound points are L and R, respectively, see Fig. 6. The vector of parameters is:

$$\boldsymbol{\alpha}_{(4\times 1)} = \{k\,(f = 0.2\ \text{MHz}), k\,(f = 0.25\ \text{MHz}), k\,(f = 0.30\ \text{MHzz}), k\,(f = 0.25\ \text{MHz}), (f = 0.35\ MHz)\} \quad (7)$$

The basis function with parameters (17) was used as a good approximation of LDCs. Selected results of the identification analysis are shown in Table 2. They correspond to the neural network MLP: 4-6-1 with one BF and MLP: 8-6-3 with two BFs.

MLP Neural networks	Number of parameters		Model, α °	Identified parameters		Relative testing errors *ReT* [%]	
	P	L		C_{ij}	MPa	max	mean
8–10–3	2541	847	A_0, S_0, 0 °	C_{11} C_{12} C_{44}	93.00 0.019 3.74	6.11 0.005 12.97	0.64 0.001 4.30
4–6–3	2541	847	A_0, 0 °	C_{11} C_{12} C_{44}	99.45 0.301 3.81	0.65 0.010 19.50	0.059 0.001 8.13
4–6–1	101	34	S_0, 45 °	C_{22}	17.46	0.049	0.003
4–6–1	41	14	A_0, 45°	C_{55}	5.62	0.158	0.008

Table 2. Identified values of stiffness constants

It is worth mentioning that the results shown in Table 2 were obtained for 100 'trained off line' networks. The computed value of the stiffness equals $C_{23} = C_{22} - 2\,C_{44} = 17.46 - 2\times3.74 = 9.98$ GPa. The stiffness C_{55} for computed for wave-number, evaluated from Fib. 4, $\alpha = 45^{o}$, for $f = 0.5$ MHz as $k \approx 1500$ m^{-1}. The stiffness value calculated by formula (16) equals $C_{55} = C_{55} \approx 8.58$ GPa.

5. SOME REMARKS AND FINAL CONCLUSIONS

- The presented paper is a continuation and development of paper [14], where the modeling and analysis are related to an isotropic material. In the presented paper the considered analysis is much more extended than in [15].
- It was proved that the main idea of the Hybrid Computational System (HCS), i.e. separation of direct and reverse analyses can be extended to the analysis of orthotropic material. This can be carried out owing to the application of Artificial Neural Networks (ANN).
- In the present paper the attention was focused on the analysis of the hexagonal model of orthotropic material, useful in the analysis of unidirectional reinforced composites.
- The search for starting values of material constants was based on the sensitivity analysis of the Lamb Dispersion Curves changes of material constants.
- The obtained results seem to be useful for the development of HCS for a numerically efficient analysis of composite plies [16].

A APPENDIX

A semi-analytical method for dispersion curves computation

The regular discrete grid was adopted for the space stations across the plate thickness, see Fig. A1. The regular grid of points is used with spacing $\{\Delta x, \Delta y, \Delta z\}$.

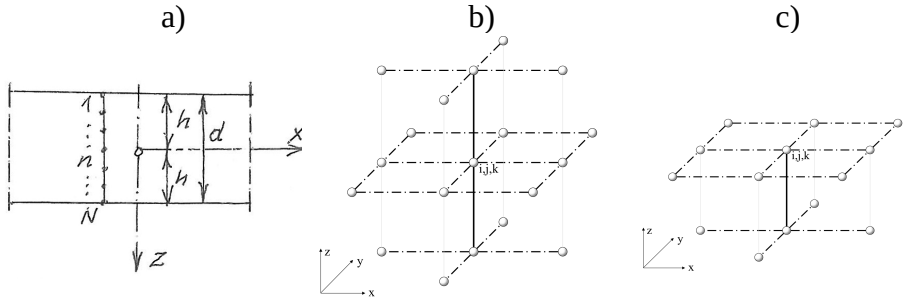

Fig. A1. a) Grid layer stations at plate cross-section, b) internal grid point c) upper boundary grid point.

At each station the elastodynamic equation is discretized. The equilibrium at a station point is given by the semi-analytical LISA equation and, following [13], and it can be expressed as:

$$-\rho_s \frac{\delta^2 \mathbf{W}}{\delta t^2} = \frac{1}{\Delta V} G(\mathbf{W}^{x_1 \pm 1, x_2 \pm 1, x_3 \pm 1}), \tag{A1}$$

where: $G(\mathbf{W})$ – function of material properties, particle displacements and discretizing parameters, ΔV– volume enclosed by neighbouring grid points, ρ_s – sum of density values for all cells surrounding the station point (see Fig. A1).

Subsequently, equation (A1) is re-formulated in the spectral domain along $x_{n=1,2}$ directions. Effectively, grid points adjacent to the considered station point, namely, $\mathbf{W}^{x_1 \pm, x_2 \pm 1, x_3 \pm 1}$ are substituted by $(\tilde{\mathbf{W}}^{(x_1, n \pm, x_2, n \pm 1, x_3 n \pm 1)} e^{\pm i k_x \Delta x \pm k_y \Delta y}$, where $\tilde{\mathbf{W}}$ denotes a discrete-space-Fourier-transformed quantity. It should be noted that the left-hand-side of Eq. (A1) is transformed as, i.e. the time remains as non-discretized (continuous) quantity. Letting $\rho_s \omega^2 \tilde{\mathbf{W}} = \chi^2_{S-A} \tilde{\mathbf{W}}$, where χ^2_{S-A} is the semi-analytical (S-A) counterpart.of $\chi = \Delta t^2 / (\rho_s \Delta V)$,we obtain:

$$-\chi^2_{S-A} \tilde{\mathbf{W}} = \frac{1}{\Delta V} \tilde{G}(\mathbf{W}^{x_3,(n-1,n,n+1)}, e^{i(\pm k_x \Delta x \pm k_y \Delta y)}), \tag{A2}$$

where indices x_n for n = 1, 2 have been omitted for brevity. Formula given by Eq. (6) is the bulk wave dispersion equation of the semi-analytical method and involves only the trans formed displacement values for $x_{3,(n\pm1)}$ grid points.

Manipulating and assembling (A2), using the scheme presented in Fig. 3, leads to an eigenvalue problem analogous to (4). The solution of Eq. (A2) provides the (k, $\chi_{S\text{-}A}$) pairs for the Lamb waves. For the definition and implementation details, the reader is referred to [10].

Acknowledgement

Authors of this paper are gratefully acknowledged, to the Polish National Science Centre, Grant No. UMO-2011/01/B/ST8/ 07210, AGH No.18.18.130.384, "Structural Health Monitoring by means of inverse problem solution under uncertainty", for financial support.

REFERENCES

[1] M.M. Ettoney, S. Alampalli. *Infrastructure Health Monitoring in Civil Engineering: Theory and Components*, vol. 12. CRS Press, Taylor& Francis Group, 2012.

[2] A. Raghavan, C.E.S. Cesnik. Review of guided-wave structural health monitoring. *The Shock and Vibration Digest*, **39**: 91-114, 2007.

[3] Ł. Ambroziński, L. Packo, T. Stepinski, T. Uhl. Ultrasonic guided waves based method for SHM: simulations and an experimental test. *The 5th World Conference on Structural Control and Monitoring* 5WCSCM, pp. 10443-10452, 2010.

[4] G.L. Rose. *Ultrasonic Waves in Solid Media*, Cambridge University Press, 1999.

[5] Z. Su and L. Ye, Identification of damage using Lamb waves: from fundamentals to applications. In F. Pfeifer and P. Wriggers (Series eds), *Lecture Notes in Applied and Computational Mechanics*, vol. 48, Springer, 2009.

[6] P. Packo, L. Ambrozinski, L. Pieczonka, W.J. Staszewski, T. Uhl. The influence of experimental and numerical parameters on the dispersion curves used for elastic constants identification. *Inverse Problems in Sci. and Eng.*, submitted for publishing, 2014.

[7] W. Ostachowicz, J.A.Gűemes (Editors). *New Trends in Structural Health Monitoring.* CISM Courses and Lectures, vol.542. Springer 2013.

[8] P. Fellinger, R. Marklein, S.Klaholz. Numerical modelling of elastic wave propagation

and scattering with EFIT – elastodynamic finite integration technique. *Wave Motion*, **21,** 47-66, 1995.
[9] W. Ostachowicz, P. Kudela, M. Krawczyk, A. Żak. *Guided Waves in Structures for SHM.* J Wiley&Sons, 2012.
[10] P. Packo, T. Bielak, A.B. Spencer, W.J. Staszewski, T. Uhl, K. Worden. Lamb wave propagation modelling and simulation using parallel processing architecture and graphical cards, *Smart Materials*., **21**, 2012.
[11] Packo, L. Pieczonka, L.Ambrozinski, T. Uhl. T 2013 Elastic constants identification for laminated composites based on Lamb waves. *Proceedings of the 9th International workshop on Structural Health Monitoring.* In: Fu-Kuo Chang (ed)., Vol 1, ISBN 978-1-60595-115-7. Stanford, September 10–12, 2010.
[12] M. Sale, P. Rizo, Z. Marzani. Semi-analytical formulation for guided waves-based reconstruction of elastic moduli. *Mech. Systems Signal Processing*, **25,** 2241-2256, 2011.
[13] P. Packo, T.Uhl, WJ. Staszewski. A general semi-analytical difference method for dispersion curves calculation and numerical analysis in Lamb wave propagation. *Journa*l *Acoust. Soc. America,* **136**, 993-1002, 2014.
[14] E. Pabisek, Z. Waszczyszyn, L. Ambrozinski. A semi-analytical method for identification of thin elastic plate parameters basing on LWM. *Computer Assisted Mechanics in Engineering Sciences*, **21**, 5-14, 2014.
[15] E. Pabisek, Z. Waszczyszyn. Identification of thin elastic isotropic plate parameters applying Guided Wave Measurement and Artificial Neural Networks, submitted for publication, *Mechanical Systems Signal Processing*., 2014.
[16] S. Pant, J. Laliberte, M. Martinez, B. Rocha. Derivation and experimental validation of Lamb wave equations for an *n*-layered anisotropic composite lamina. *Computers & Structures,* **111**, 566-579, 2014.
[17] V. Amirkulova. *Dispersion Relations for Elastic Waves in Plates and Rods*. M. Sc. Thesis. The State University of New Jersey, 2011.
[18] Lei Wang, FG. Yuan. Group and characteristic wave curves Lamb waves in composites: Modeling and Experiments. *Composite Science and Technology*, **67** 1370-1384, 2007.
[19] Z. Waszczyszyn, Artificial neural networks in civil and structural engineering: ten years of research in Poland, *Computer Assisted Mech. in Eng. Sci.*, **13**, 489-512, 2006.
[20] Z.Waszczyszyn, Artificial neural networks in civil and structural engineering: another five years of research in Poland, *Computer Assisted Mechanics in Engineering Sciences*.,**18**, 131-146, 2011.
[21] GR. Liu, KY. Lam, X. Han. Determination of elastic constants of anisotropic plates using elastic waves and a progressive neural network. *Journal of Sound Vibrations*, **252**, 239-259, 2002.
[22] D. Alleyne, P. Cawley. A two-dimensional Fourier transform method for the measurement of propagating multimode signals *The Journ. Acoust. Soc. America* ASA. **89:** 1159-1168, 1991.
[23] S.Haykin, *Neural Networks: a Comprehensible Foundations*, 2nd ed., Prentice–Hall, 1999.